Received: 20 December 2021 | Revised: 14 June 2022 | Accepted: 9 August 2022

DOI: 10.33012/navi.560

ORIGINAL ARTICLE

Radio-Frequency Interference Considerations for Utility of the Galileo E6 Signal Based on Long-Term Monitoring by ARFIDAAS

Aiden Morrison[1] | **Nadezda Sokolova**[1] | **Nicolai Gerrard**[2] | **Anders Rødningsby**[3] | **Christian Rost**[4] | **Laura Ruotsalainen**[5]

[1] SINTEF AS

[2] Norwegian Communications Authority

[3] Norwegian Defence Research Establishment

[4] Norwegian Space Agency

[5] The University of Helsinki

Correspondence
Aiden Morrison,
SINTEF AS
Strindvegen 4, 7034 Trondheim Norway
Email: Aiden.Morrison@sintef.no

Abstract

The extent to which navigation signals in the E6 band may be impacted by shared spectrum allocations might be underappreciated. This paper presents top-level observations from a multi-year international radio frequency interference (RFI) monitoring project covering all L-band global navigation satellite system (GNSS) signals with specific focus on the challenges facing the E6 band. The context of this paper is the assumption that most users will be non-authorized and have access to only the open data-bearing signal component and not the encrypted pilot of the E6 Galileo signal. In virtually all locations where the Advanced RFI Detection, Analysis, and Alerting System (ARFIDAAS) monitoring stations were deployed, frequent disruption of the E6 band from systems such as radar installations or other authorized users of the spectrum was observed. In the presented paper, an effort is made to put the observations in the context of the expected use cases of the E6 signal.

Keywords

GNSS, E6, jamming, radio-frequency interference

1 | THE ARFIDAAS PROJECT BACKGROUND AND SYSTEM DESIGN

The Advanced RFI Detection, Analysis, and Alerting System (ARFIDAAS) is a European space agency navigation, innovation, and support program (NAVISP) Element 3 initiative started in 2018, focusing on the capture and collection of radio-frequency interference (RFI) events impacting GNSS L-band signals. One of the key features of the ARFIDAAS project is that it utilizes custom monitoring hardware front-ends to simultaneously observe at least 240 MHz of aggregate spectrum divided into four tunable sub-bands. The typical configuration is of one covering the L1 band including BeiDou B1 through GLONASS G1 signals, and the other three partially overlapping bands spread between the Galileo E5a+E5b, GPS L2, and Galileo E6 signals.

The primary motivation for developing ARFIDAAS was that the state of the art of previous GNSS RFI monitoring campaigns had limitations in the context

of spectral coverage as well as data retention and availability. For example, the European Union (EU) Horizon 2020 project, STRIKE3, produced the largest previously known compilation and analysis of observed RFI events from 2016 through 2019, comprising more than 450,000 events (Towlson et al., 2019). Unfortunately, the design of the STRIKE3 system hardware allowed for observation of only a portion of the L1 band at most stations with an optional coverage of the L5 band, leaving other portions of the spectrum unobserved. Additionally, the STRIKE3 network did not centrally collect captured event data nor provide for public availability of this data past the conclusion of the project term. In order to avoid these shortcomings, while also allowing multi-site deployment at a reasonable cost level, ARFIDAAS was purposely built for the application of monitoring all active GNSS L-band signals and the central aggregation of all captured events.

The ARFIDAAS hardware is comprised of a purpose-built front-end design by and for the ARFIDAAS project members that allows simultaneous coverage and capture of all present GNSS L-band signals from all operative constellations while also providing data streams specifically selected to aid in the tasks of detection and characterization of both unintentional RFI events and malicious jamming activity, along with a commercial-off-the-shelf (COTS) host computer and a connected GNSS antenna. To minimize the amount of computational power required for the host system, the front-end directly provides in-band power measurements and automatic gain control (AGC) state information to the host system in each packet header, allowing these parameters to serve as pre-detection gates and eliminating the need to process the full output of the ARFIDAAS front-end in real time. The signal-handling sections of the front-end shown in Figure 1 are designed to tolerate the maximum signal power that can be represented by an active antenna when the 5-volt internal bias voltage optionally generated by the front-end is used to power the antenna low noise amplifier (LNA). Alternatively, the front-end can also tolerate high reverse biasing voltages as a precaution against being connected to an externally biased network without a direct current (DC) block. The onboard oscillator is an oven-controlled crystal oscillator (OCXO) that provides a stable phase reference for RFI signal analysis. The reference oscillator is made available on an external subminiature version A (SMA) connection to optionally drive external equipment synchronously. Alternately, an external 10-MHz signal may be fed into the front-end to drive it instead of the onboard oscillator. On the digital side of the design, the system field-programmable gate array (FPGA) communicates via a USB3 first-in-first-out (FIFO) from which command packets for the configuration of the

FIGURE 1 ARFIDAAS second-generation hardware front-end

front-end parameters are received, while packets containing collected samples and metadata (e.g., bit bin populations, AGC parameters, measured in-band power meter outputs, current configuration parameters) are streamed to the host system. While both the original and second-generation ARFIDAAS front-ends handle four-bit quantization internally for AGC feedback, the output of the first-generation system was limited to three-bit quantization at 60 MHz complex for a total of 180 MB/second of data, while the second-generation hardware is capable of four-bit quantization at 75 MHz for 300 MB/second of data.

Design elements of note that assist in the objective of GNSS RFI monitoring include a dual surface acoustic wave (SAW) filter input configuration that excludes all non-GNSS bands. In addition, the filter splits the input signal in to an L1-band channel fed to one mixer and one in-band power meter, and a second channel fed to three mixers and a second in-band power meter to allow independent lower and upper L-band power observations. The mixing and down conversion stages apply additional filtering to the intermediate-frequency (IF) data to help the system ignore adjacent band interference from signals that pass the antenna and first stage SAW filtering, but are not in the band targeted by a given mixer. The in-band power measurement sensors allow the ARFIDAAS to accurately assess relative changes in the local radio-frequency (RF) environment independent of the modulation of the encountered RFI signals. This is in contrast to solutions that rely only on the carrier-to-noise density ratio (C/N_0) or AGC feedback monitoring-based power level assessment, while also supporting a wide variety of installation environments.

The software and cloud interfaced portions of the ARFIDAAS design are shown in Figure 2. The software of ARFIDAAS is designed to provide essential event data to site operators at low latency, as well as comprehensive information to shared cloud storage to enable both immediate reactions to RFI when necessary as well as complete event data for later centralized analysis. The detection software deployed on each node is configurable via a web interface to allow site operators to define the characteristics of the RFI that they wish the system to detect and report. User configurable detection settings include the magnitude of in-band power deviation and the duration for which it must persist, and the rate at which both in-band power and AGC thresholds are allowed to vary to account for factors such as thermal variation in the antenna LNA. Parameters for the data to be captured include the duration of raw RF data to be saved during a detection event, whether AGC deviation is required in the given band, or if events in certain bands should be reported but not uploaded to the cloud. Additional options include both the email addresses to be notified during detections, and the limitations to usable instantaneous and monthly upload bandwidth that the system should respect.

After initial notification emails are sent with rapidly generated spectrogram and waterfall plot contents, a source classifier algorithm is run on the edge computer which attempts to categorize the type and primary signal characteristics of the detected event (e.g., continuous wave, chirp, multilevel chirp, other wideband). For example, when a chirp event is detected and classified, the total sweep range and sweep rate are also determined and noted along with the center frequency of the RFI and the impact in terms of power level deviation relative to baseline. When the system is unable to determine a specific modulation type for the signal, it will fall back to generalized categorization including narrowband general, wideband general, and baseline variation. The latter is an indication that anomalous power and AGC feedback deviation has been detected in-band at or above the levels specified by the site operator, but that the event is either too weak or too evenly spread over the band to be isolated. Once local event analysis has completed collection of the raw RF datafile package, generated visualization documents, initial event report

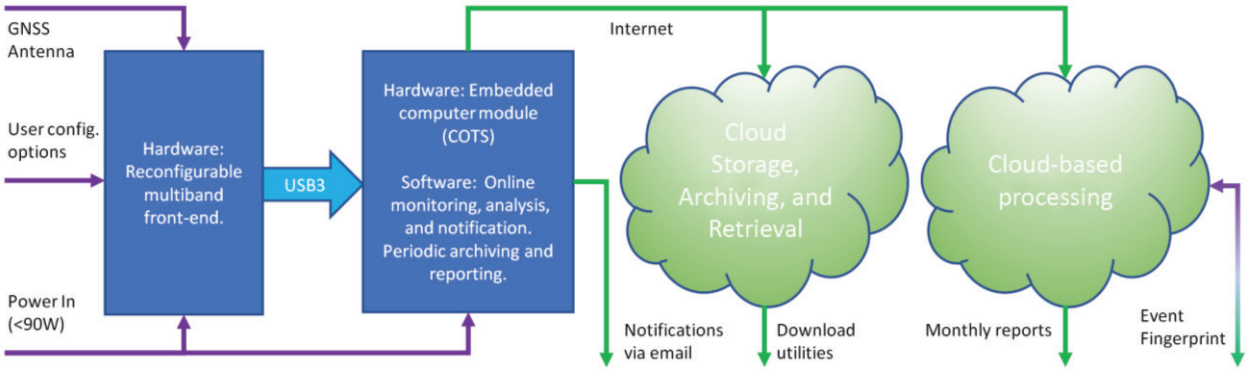

FIGURE 2 ARFIDAAS high-level functional diagram showing interfaces

text file, and the event classifier results database file are collectively uploaded to centralized cloud storage. Data collected in the centralized cloud storage now exceeds 20 TB of multiband reference material making the ARFIDAAS database the largest known open-access repository of raw GNSS RFI and jamming event data. The collection of this large volume of data sorted by site and date allows for the production of detailed site report summaries, typically at time resolutions of one month or one year to allow characterization of the site RFI environment and to identify trends in the number and type of jamming devices encountered at each over time. By the end of the project in 2022, it is planned to provide site stakeholders and interested parties with monthly and annual reports for deployed stations as well as to allow machine-learning-based fingerprinting of detected jammers such that individual hardware devices can be recognized and their previous sightings over the whole catalogue of events can be reported.

2 | THE DEPLOYED ARFIDAAS NETWORK

As of the writing of this paper, there are 11 deployed ARFIDAAS monitoring stations throughout Scandinavia and Europe, with plans for an additional six units to be deployed within 2022, as detailed in Morrison and Sokolova (2021). The ARFIDAAS network is hosted primarily by cooperating research institutions and organizations with active research or development projects utilizing GNSS signals. Typically, ARFIDAAS is connected to an existing GNSS multiband antenna via a signal splitter shared with receivers and equipment operated by the host. In order to support the use of dissimilar antennas and RF feed networks between the different host locations, the ARFIDAAS hardware front-end was designed to support a very wide signal power range and to tolerate reverse biasing from DC injection on existing networks. Similarly, to allow ARFIDAAS to integrate into available installations, several configurable aspects of the ARFIDAAS configuration software are used to suit the given site.

First, detection is based on deviation from a slew-rate limited moving baseline rather than a static threshold of signal amplitude, which eliminates the need for calibration while also tolerating gain variation within the antenna and signal propagation network that can arise from temperature variation. Second, the center frequencies, IF bandwidths, and sampling rate parameters can each be adjusted to tailor the amount of captured spectrum to the signal bands and bandwidths supported by the connected antenna. Third, the system software allows for some masking of nuisance events either in terms of reporting, uploading, or both in cases where sites are found to suffer from the presence of a persistent yet unstable in power co-authorized user that would otherwise cause frequent nuisance detections.

3 | KNOWN CHALLENGES TO THE USE OF E6 AND ARFIDAAS FIELD OBSERVATIONS

It is well understood that the E6 band is neither dedicated to GNSS alone nor to aeronautical radio-navigation service (ARNS) systems exclusively, and that the rights of pre-existing users in various jurisdictions can allow the presence of high-pulsed or continuous power signals in bands overlapping the main lobe of the E6 signal. In de Bakker (2007) and Arribas et al. (2019), the authors present a partial listing of signal types known to be potential sources of interference to the E6 band, including but not limited to radar, while Van Hees (2016) expands the list with specific examples of other harmful sources including security cameras from China and amateur TV in Germany. While the camera example given is believed to be illegal in most jurisdictions, the German amateur TV signal is legal yet fits the criteria of a jammer of E6 due to the signal having substantial bandwidth (multiple MHz) overlapping the main lobe of the E6 signal and continuous transmission at a relatively high-power level.

A separate report dealing with the potential availability impacts to E6 on German roadways in Schütz et al. (2021) concludes that, in the worst case, amateur radio interference could prevent use of signal on the majority of the national highway network in Germany. While the ARFIDAAS has not yet deployed to Germany, several sources of E6 RFI from co-authorized users of the spectrum have been observed in other nations (Morrison et al., 2021). An unfortunate consistent observation between deployment sites has been the prevalence of nuisance signals within the L2 and E6 bands, which have ranged from occasional observations at some sites to persistent disruptions at others. Due to the detection method of the ARFIDAAS being sensitive to variation in local power levels, a strong continuous transmission source will be ignored while an unstable or intermittent one will appear as events of interest. Below follow several examples of such nuisance signals observed in field.

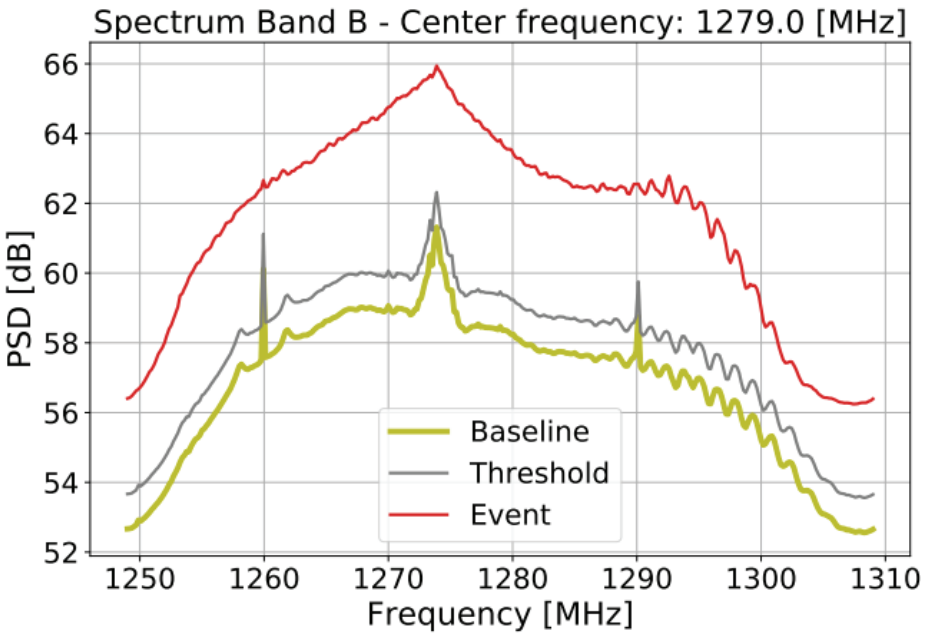

FIGURE 3 Example of interference assumed to be radar-related jamming events from Norway on the 19th of January 2021 (not showing leakage into the L2 band)

3.1 | Radar Installations and Electronic Warfare Exercises

In Helsinki, a radar installation would trigger the system so frequently with spurious signals near GLONASS L2 and BeiDou B6 that low band detection had to be turned off entirely to prevent tens of daily detections based on these nearby transmission sources. The user software has since been updated to allow selective band masking of events to allow operation in similar conditions without flooding the event database.

Multiple other sites within Norway are subjected to not only continuous in-band power due to proximity to primary radar sites as shown in Figure 3, but more troublingly, their associated emissions which appear to be (legal) radar-jamming tests. As an example, the primary radar site near Trondheim uses a center frequency of 1,272 MHz, placing it almost directly on the main lobe of E6. The RFI emissions that are assumed to be used for testing the radar have been observed covering from the top end of ARFIDAAS reception at 1,300 MHz down through 1,200 MHz and the associated E5b signal.

Other sites, such as one recently installed in the Czech Republic, show a potential radar installation operating near 1,289 MHz, as shown in Figure 4. This installation appears to have better spectral separation from the E6 main lobe, though it may still be a challenge to receivers operating in close proximity and may be causing intermodulation effects to appear within the L2 and E5 bands as well. It should be noted that this impact is observed when using an antenna that has a nominal pass-band extending only to 1,254 MHz.

Some of the events observed are assumed to be related to parts of pre-announced electronic warfare tests (Lynum, 2020), and manifested as regular two-hour periods of activity spanning Monday through Friday interspersed with quiet periods. Other tests are both unannounced and follow no apparent schedule. In light of the frequent and widespread impacts to signals in the E6 and upper L2 bands, it is appropriate to reconsider some of the recent publications discussing the signal tracking challenges (Borio & Susi, 2019; Curran & Melgård, 2016; Susi & Borio, 2020) faced

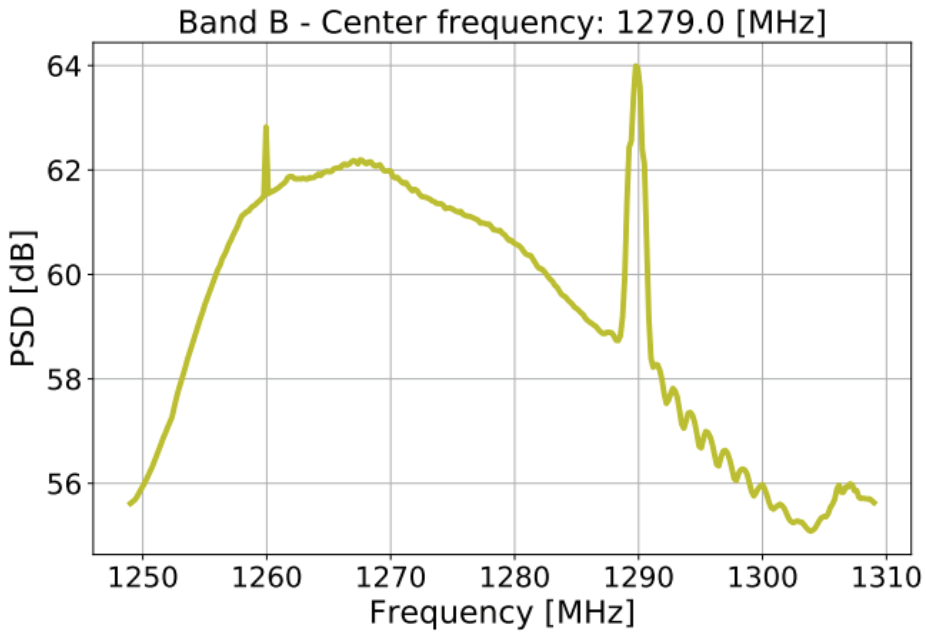

FIGURE 4 Czech Republic installation environment baseline of E6 band

by E6 civil receivers through the lens of potential electromagnetic interference (EMI) presence.

3.2 | Narrowband Amateur Radio

In many European countries, including the Netherlands, it is legal to use portions of the E6 band for amateur radio purposes. While these amateur radio transmissions are narrowband and not typically overlaid on the main lobe of the E6 signal, which mitigates their impact on the GNSS signal tracking, the power level of the amateur radio signals can be extremely high. In the case of the ARFIDAAS station in Amsterdam, the center frequency of the second of the four channels, Band B, had to be migrated down from 1,279 MHz to 1,267 MHz, and the IF pass-band filter width reduced from greater than 55 MHz to less than 30 MHz to prevent the system from triggering due to narrowband transmissions near 1,294 MHz. When the source of this transmission was identified, it was determined that the site operator was employing an amplifier rated for 300-Watt output connected to a high-gain dish antenna coincidentally pointed towards the site where the ARFIDAAS station was installed. While it is not believed that the site operator was transmitting at full power, their transmission was still sufficiently strong to overwhelm signal reception in the E6 band despite the GNSS antenna in use at that site not nominally supporting E6 reception and the offending signal being well into the antenna filter roll-off domain.

3.3 | Malfunctioning Wi-Fi Routers

In Trondheim, Norway, one site with an antenna pointed laterally to cover a busy freeway also covered a residential neighborhood with the main lobe of the monitoring antenna. Somewhere within the residential area, a strong signal below E6 covering parts of the side lobes and GLONASS G2 would trigger multiple daily detections, necessitating the deactivation of low band sensitivity during initial operation of the station. In 2021 when similar signatures appeared on other stations in Trondheim, it was decided that finding the source was a priority. The Norwegian communications authority was able to localize three or more sources responsible for this RFI, each of which proving to be from malfunctioning Wi-Fi routers. All three routers were the same model of device from a reputable manufacturer that was legal for sale in the EU and Norway, but all had apparently developed a fault or possessed a manufacturing defect that caused them to leak a significant amount of energy at half of their nominal operating frequency such that they were detected by ARFIDAAS monitoring stations hundreds of meters distant and through building walls.

3.4 | Satellite-Borne RFI Sources

An unexpected source of E6 RFI is believed to be from a synthetic aperture radar (SAR) payload carried on board the Advanced Land Observing Satellite 2 (ALOS-2) that manifests as low duty cycle but extremely high peak power chirps as shown in Figure 5. This source was first noted in the summer of 2021 when multiple ARFIDAAS stations separated by hundreds of kilometers detected the same spectral signature within a few minutes of each other, indicating that this was either

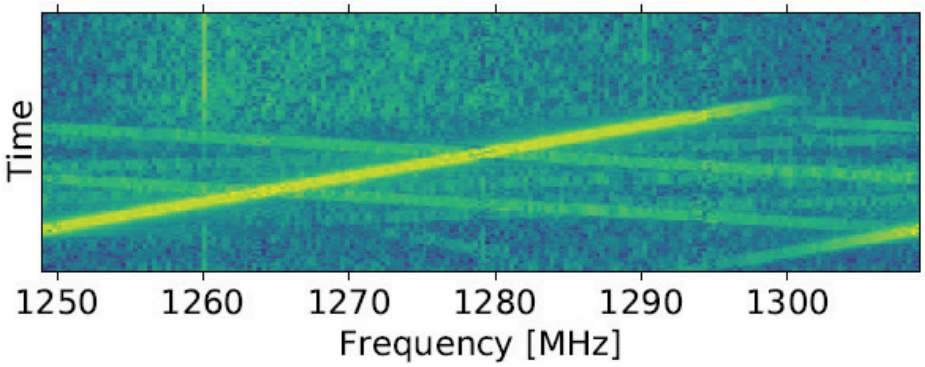

FIGURE 5 E6-band disruption believed to be from the SAR payload of the ALOS-2 satellite

a coincidental detection or that the source was in a low Earth orbit satellite. By collecting multiple observations of the phenomenon and comparing them with satellites that were visible at the time of the reception, it was noted that the ALOS-2 satellite, which occupies a sun-synchronous orbit, was a common factor. Publicly available documentation indicates that the satellite carries a 1–2 GHz SAR system, which is a very likely candidate for being the source of the detected signal.

This signal is more commonly observed within the GPS and GLONASS L2/G2 bands, but simultaneously impacts the adjacent E5 and E6 bands due to saturation effects stemming from the sharing of a single wideband SAW filter for all of these lower bands within the ARFIDAAS front-end hardware. In this specific instance, the signal was centered at a higher midpoint around 1,270 MHz (JAXA, 2014), overlaying the E6 signal main lobe. While this is not a common occurrence, it was a novel and unexpected source of intermittent tough and potentially global E6 RFI.

3.5 | Frequency Shift Keying (FSK) Amateur Radio and Amateur TV Broadcast

While ARFIDAAS stations in the Netherlands have detected narrowband amateur radio in the E6 band, we have not to our knowledge detected higher bandwidth amateur radio or TV signals that might be expected to disrupt the E6 band in other countries. Recent publications from Germany including Schütz et al. (2021) indicate that the coexistence of amateur radio at 1,291 MHz is unlikely to respect the 1-dB criteria in terms of expected impact on the E6 signal over much of German territory. Simultaneously, the authors of this publication dismiss the coexistence of amateur TV signals and E6 as effectively impossible. The challenge to E6 use in these cases may rely on the eventual migration of these signals to other bands, but this appears unlikely to occur in the foreseeable future.

4 | FULL-YEAR SITE STATISTICS

While anecdotal observations can help to bring light to problems, we now turn to the long-term site monitoring produced by the ARFIDAAS network to determine the actual absolute and relative likelihood of RFI being experienced by GNSS signals at a given site. For this purpose, full-year periods of detected RFI data from the five stations shown in Table 1 have been collected and postprocessed by event analysis software that attempts to extract detailed information about the modulation and characteristics of the detected RFI events.

TABLE 1
Full-Year Results From Five ARFIDAAS Monitoring Stations

Site name	Number of events	Most impacted band	Likelihood of jamming at site		Dominant RFI family
			in %	seconds/day	
Amsterdam	2,291	E1/L1	0.025	22	Narrowband
Asker	1,295	E1/L1	0.016	14	Wideband
Trondheim	3,021	E6	0.024	21	Time-modulated
Trondheim B	827	E1/L1	0.009	8	Time-modulated
Trondheim C	5,110	E1/L1	0.042	36	Narrowband

One of the first important parameters that can be extracted from the full-year data sets is the likelihood of experiencing RFI conditions at the site in question which is expressed here as the proportion of time during which the station is impacted by RFI exceeding the power level and AGC thresholds specified over the monitored period in both percentage and as an equivalent number of seconds per day. Contextualizing the importance of a given level of RFI occurrence is highly dependent on the use-case scenario, with a rate of a few tens of seconds per day being absolutely inconsequential for recreational uses, location-based services, and even survey applications when the periods of disruption do not align with measurement windows. In other use cases, this same level of observed RFI is unacceptably high. For example, a GNSS-based safety-of-life navigation system such as the Ground Based Augmentation System (GBAS) operating as an instrument landing system (ILS) look-alike mode has extremely stringent requirements. The ILS look-alike availability requirement is between 0.99 and 0.99999, the continuity risk requirement is of less than two parts per million per fifteen seconds, and the integrity risk is better than one part per billion per 15 seconds as documented in Schuster and Ochieng (2010). While the GBAS leverages multiple distributed ground-based antennas and extensive monitoring of signal quality to help meet these extremely tight requirements, locations where the siting is constrained to be near busy roadways may not meet their availability or continuity requirements without onerous mitigation and siting changes as was the case at Newark airport (Pullen et al., 2012). The figures presented in Table 1 are believed to be cause for concern for any application of GNSS where denial of the GNSS signal can result in damage to the platform, property, or personnel, as well as for applications with high (greater than 99.9% in this context) availability requirements. While these levels of RFI activity are, at worst, an inconvenience for a user of GNSS only interested in location-based services, pedestrian, or in-car navigation, they are a reason for concern in the context of safety-of-life applications. Even if a system that uses GNSS for high-integrity applications is properly designed to prevent propagation of hazardously misleading information (HMI) in a GNSS-denied environment, it is possible that the consequences for continuity and availability of the service may still be unacceptable at these levels of interference.

The likelihood of jamming at a site given in Table 1 is a slightly conservative figure due to the way the ARFIDAAS uses received power level variation with an adaptive threshold to intentionally exclude (after a user-configurable adaptation/desensitization period) persistent continuously active sources such as a vehicle-borne personal privacy device (PPD) left active in a parked car near the monitor station. This adaptive threshold works by defining slew rates in dB per minute and AGC step count per minute at which the threshold values for in-band power measurement and AGC feedback state are allowed to adapt to a measured level above or below

the current threshold value. Power level and AGC feedback state moving averages are calculated over the defined detection interval and updated with each packet header from the front-end. One such persistent source event occurred in 2021 and another in early 2022 which were confirmed and dealt with by the Norwegian Communications Authority. Since the latter of these two events falls outside of the window of reporting, the second event is not included in the statistics presented in Table 1 as it would become the dominant source and modulation type at that site over the annual period due to the latency between initial onset and apprehension. Since different GNSS applications are recognized to have widely different concerns with respect to aspects of the RFI which they might experience such as modulation type or bandwidth, relative power level, and specific portions of the spectrum impacted, the software under development for producing monthly and annual reporting data will, within 2022, allow exclusion of other events from developed reports. For example, exclusion of arbitrarily weak narrowband interference sources or wideband signals that do not overlap the main lobe of a selected modulation will be allowed. The data presented here includes all events detected except for the single aforementioned parked source.

A second important aspect exposed by the long-term data in both Table 1 and Figures 6 through 10 is the universally higher occurrence rate of narrowband RFI events in the E1/L1 band than in the other GNSS bands at all of the selected sites. The working theory for this observation is that malfunctioning low-cost GNSS receivers with active antennas tend to be single frequency receivers, and therefore leak RFI or become self-resonant in this band. This prediction can be tested by watching the trend in the annual data as more multi-frequency low-cost receivers enter the market. If this assumption is correct, then we can expect to soon see increasing rates of narrowband RFI in the E5b and L2 bands where lower cost multi-frequency receivers are becoming increasingly available. It should be noted that events classified as *environment baseline* activity are those where the detected event matched the power level, AGC feedback, and duration requirements to declare that an RFI event was occurring, but the analysis software was unable to detect or classify the offending signal or changes in the captured spectral shape. While such events could, in concept, be caused by well-executed spoofing attacks, it is believed that the vast majority of these cases are due to coincidental variation in the signal power level reaching the front-end due to LNA gain fluctuations unrelated to received signals.

4.1 | Event Classification Process

Once an event has been captured and reported to the site stakeholders, it is classified on the edge computing system prior to upload to cloud storage. The classifier system is detailed in Diez et al. (2022a) and is designed to simultaneously parameterize and classify the detected RFI event(s) by extracting nine signal parameters, executing a true-false comparison versus a defined threshold within each of these signal parameters, then comparing the vector of true-false results against a classification matrix. This approach was selected based on the limited computational and memory resources on the edge units. Specific parameters evaluated include:

- The first parameter is the bandwidth of the dominant signal component.
- The second parameter is the variation of the center frequency of the dominant component over a defined fraction of the data set.
- Parameters three through six concern the presence, number, and spectral relationship between potential resonant peaks of the dominant signal.

- Parameter seven considers the presence or absence of multiple narrowband signals.
- Parameter eight compares the ratio of the short-term to long-term spectral occupancy of the signal.
- Parameter nine compares the variability of the ratio of the short-term to long-term spectral occupancy of the signal to a threshold.

In ideal conditions of controlled lab testing when evaluated against known events generated using a GNSS hardware simulator, the detector achieved a correct classification rate of 0.94 with the misclassified signals still falling within the correct parent category *time-modulated general*. When operated based on real-world data where non-idealities such as multiple distinct RFI signals are present simultaneously, signals exhibit strong power level variation over time or are very weak, or signals span multiple signal bands, thus the definition of *correct classification* is complicated. Additional information on the categorization process in the context of live RFI events with complicating factors is discussed in Diez et al. (2022b).

4.2 | Event Type and Band Distributions

Of the five sites observed, the E1/L1 band was the most impacted by RFI at four of the stations over the full year of monitoring. RFI in the E6 band was the most common of the monitored bands at one of the stations while it was the second-most frequently impacted band at two of the other stations. While it is not obvious from Figures 6 through 10, the relative occurrence rate of all bands of RFI from the

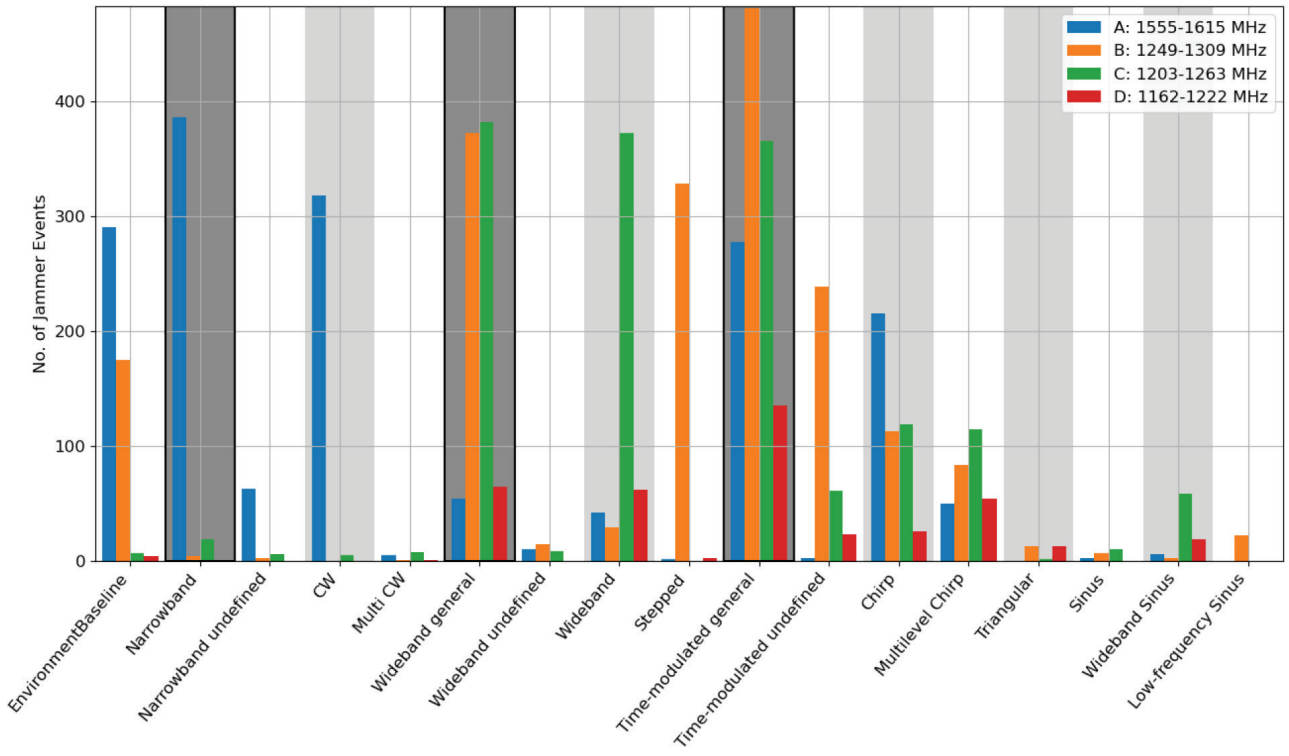

FIGURE 6 Classification results from Trondheim station: 3,021 events from January 1, 2020, through December 31, 2020

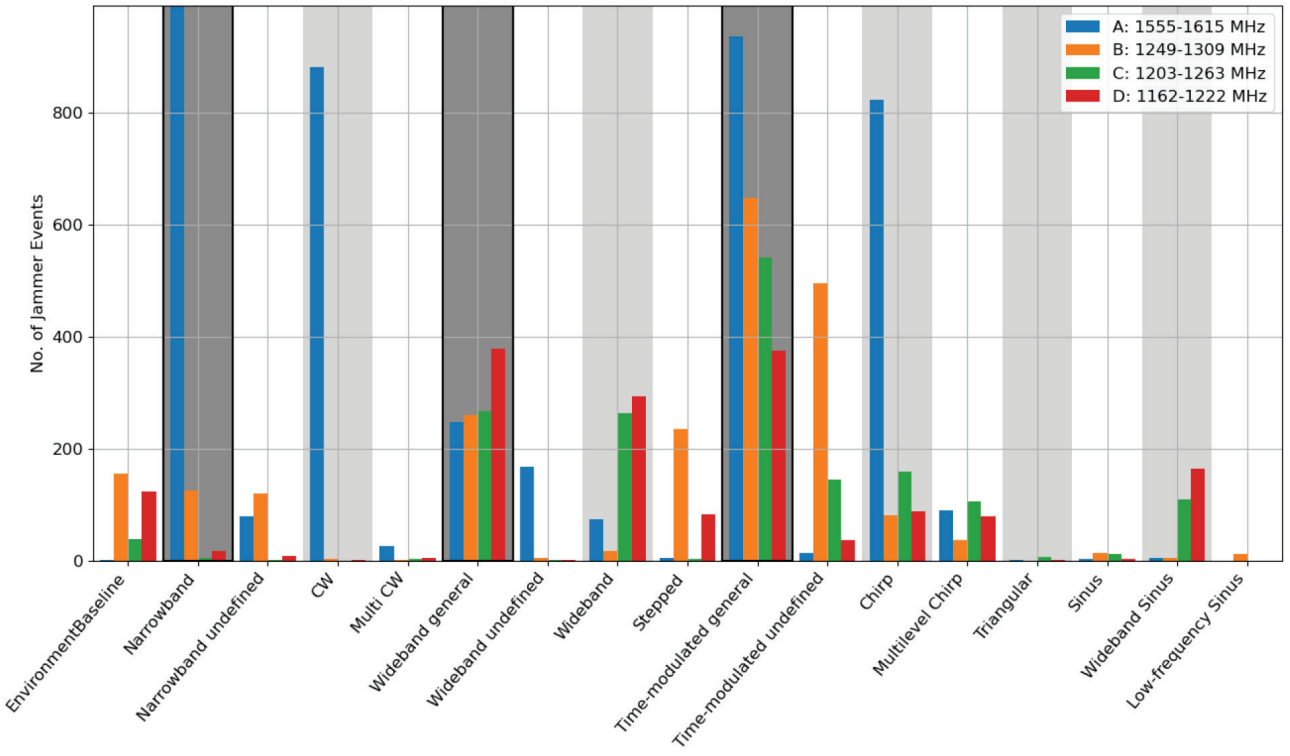

FIGURE 7 Classification results from Trondheim C station: 5,110 events from April 1, 2020, through March 31, 2021

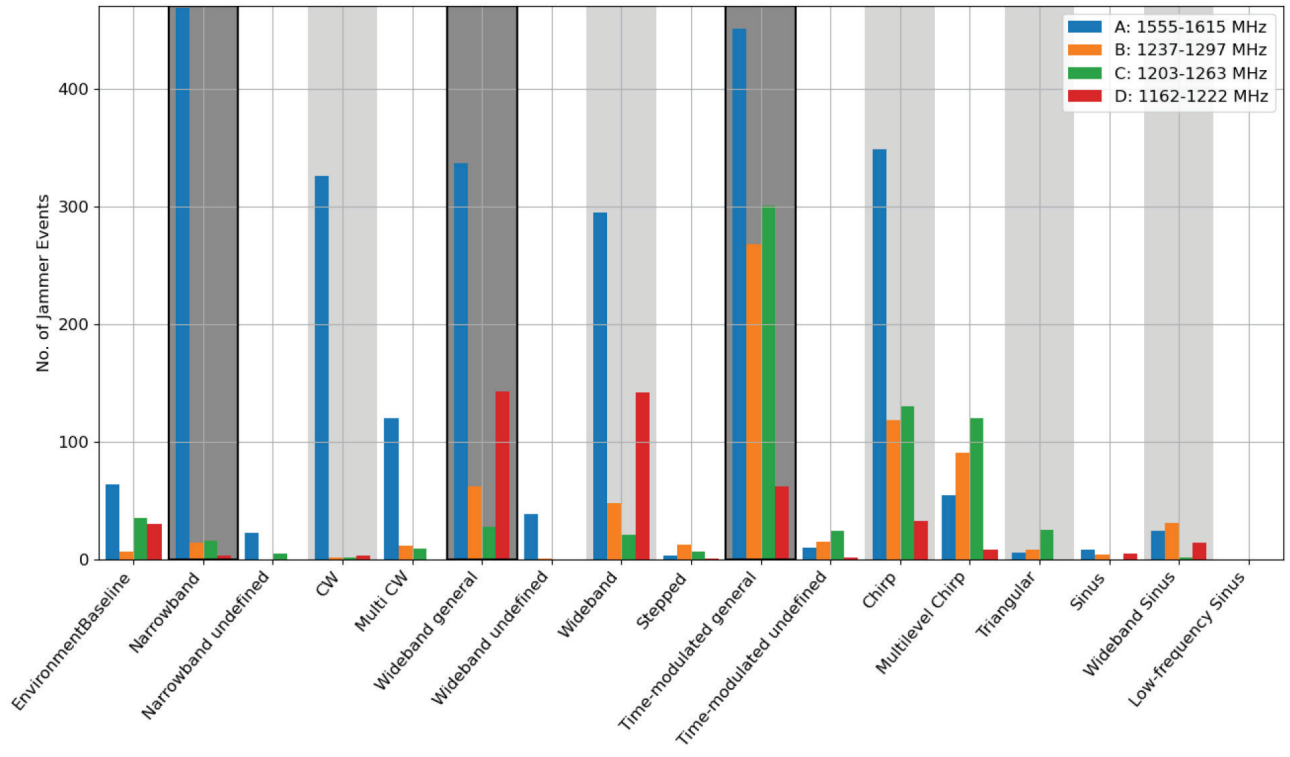

FIGURE 8 Classification results from Amsterdam station: 2,291 events from January 1, 2020, through December 31, 2020

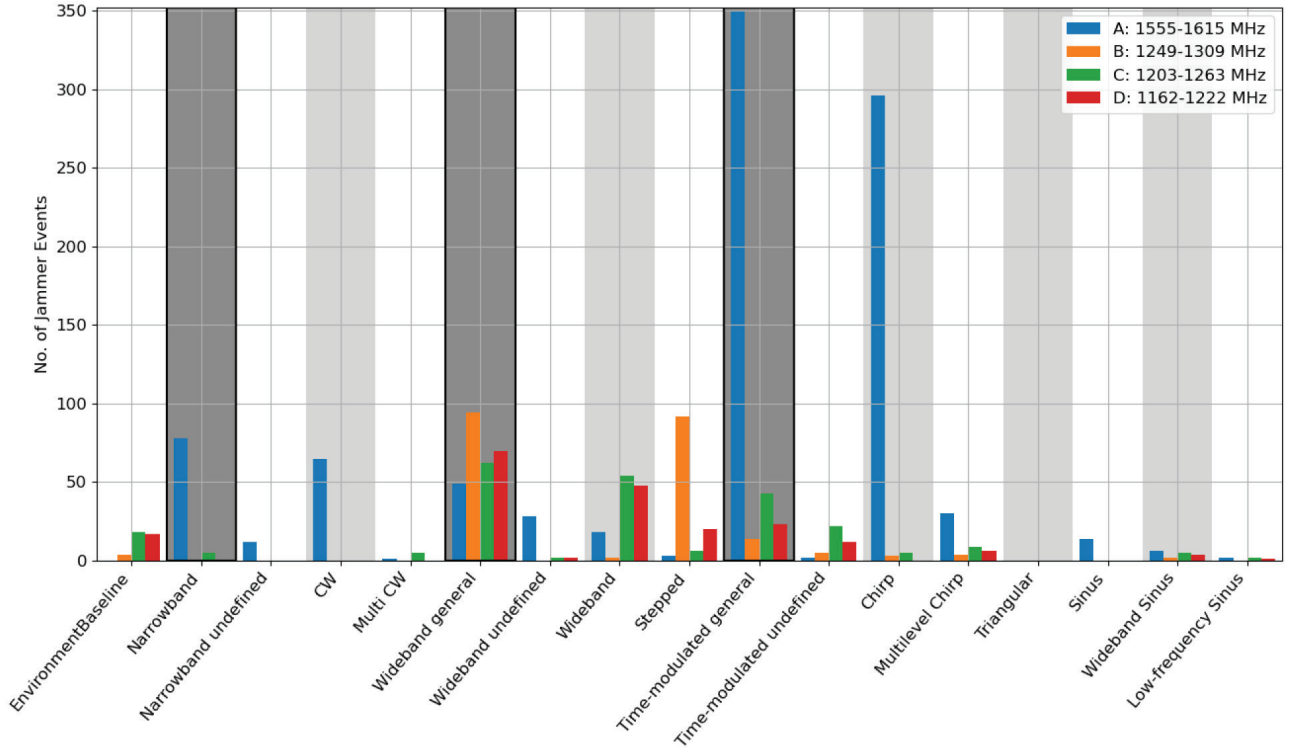

FIGURE 9 Classification results from Trondheim B station: 827 events from January 1, 2020, through December 31, 2020

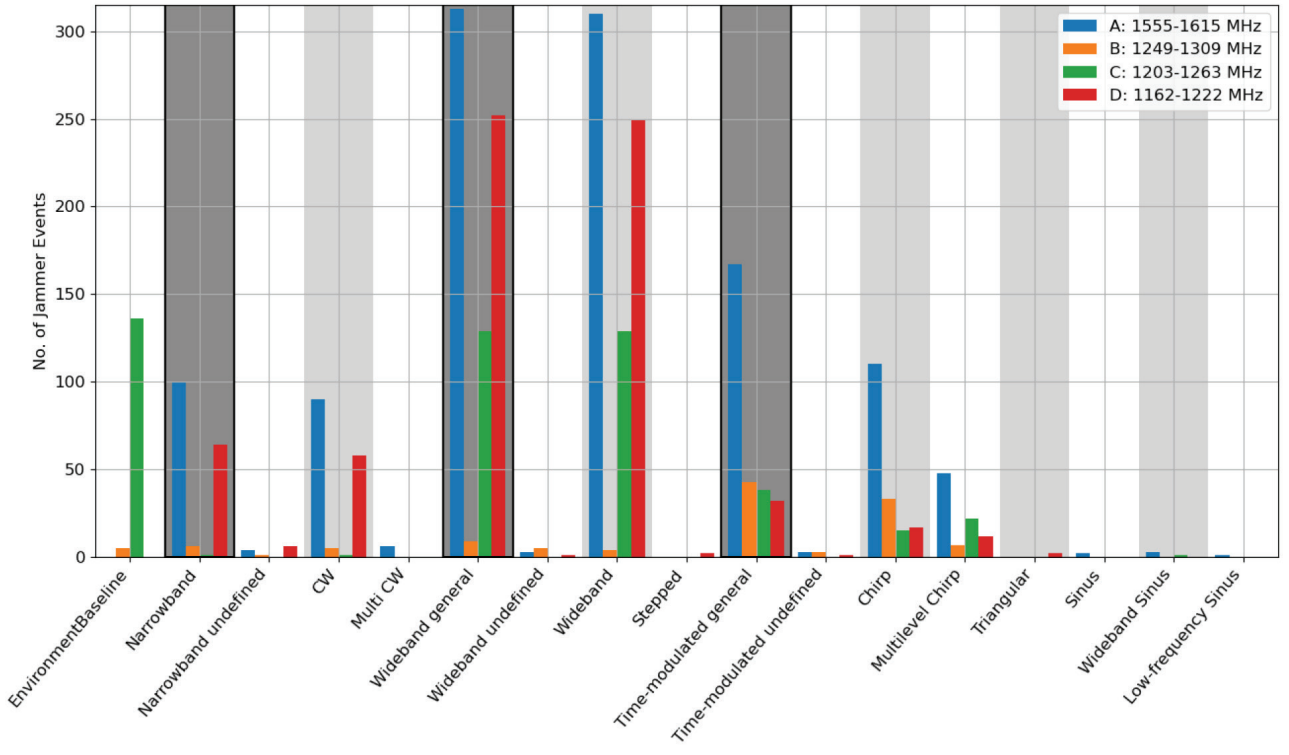

FIGURE 10 Classification results from Asker station: 1,295 events from January 1, 2020, through December 31, 2020

five selected stations tends to fall within a single order of magnitude as shown in Table 1. Given that intentionally generated RFI (e.g., chirp jammers) impacting any of the E5a, E5b, L2, or E6 bands tends to also impact the L1/E1 band, this means that receiver design approaches relying on uncorrelated RFI (e.g., frequency fallback or inter-frequency aiding strategies) may not produce the desired results. In Figures 6 through 10, parent categories are highlighted with a dark gray background and include the child categories to their right. For example, the narrowband parent category contains each of the narrowband undefined, continuous wave (CW), and multi-CW categories.

The distinction between the *wideband* and *time-modulated* signal families is primarily related to the instantaneous behavior of the received signal, where the time-modulated family tends to have well-defined frequency span and center points at a given epoch (e.g., a chirp) while wideband-classified signals occupy an arbitrarily wider span of spectrum at the microsecond level timescales used for analysis.

5 | E6 TRACKING IMPLICATIONS

Over the past 15 years of development, the exact contents and purpose of the various Galileo signals have changed, but the frequency diversity benefits discussed by Julien and Macabiau (2006) remain, as do the known and discussed drawbacks of the use of non-ARNS spectrum and adjacency or overlap with military radar.

While Julien and Macabiau (2006) focused on the benefits of the possibility of an additional carrier-phase measurement, the E6 signal structure poses significant challenges to signal tracking within receivers. As shown in Table 2, the E6 power budget is comparable to the other Galileo signal carriers, however, the structure of the E6 signal is substantially different in two important ways. First, the pilot component of the E6 signal is intended for authorized access only and will therefore not be available for the tracking of the composite E6 signal as might be done with E5 and E1 signals. Second, the symbol rate of the data-bearing component of the E6 signal is 1,000 symbols per second, limiting the allowable window of coherent integration time to one millisecond or less.

Curran and Melgård (2016) investigated the potential use of the E6 signal, implementing the proposed encrypted pilot plus high symbol rate data channel and elaborated on the signal tracking challenges faced by non-authorized users of E6.

TABLE 2
Comparative E6 Signal Structure, Power Level Symbol Rates, and Pilot Availability From the Galileo OS SIS ICD Version 2.0 (EU, 2021)

Signal	Signal component	Total received power		Symbol rate	Pilot
		Minimum (dBW)	Maximum (dBW)		
E5	E5a (total I+Q) (50/50% I/Q power)	−155.25	−150.00	50	Open
	E5b (total I+Q) (50/50% I/Q power)	−155.25	−150.00	250	Open
E6	E6-B/C (total B+C) (50/50% B/C power)	−155.25	−150.00	E6B-1000	None Requires CE6-C
E1	E1-B/C (total B+C) (50/50% B/C power)	−157.25	−152.00	E1B-250	None Open

According to this work, when the data-bearing component of the E6 signal is used by non-authorized receivers, the signal will be of limited use to users who expect to frequently encounter significant dynamics due to the lower tracking margins this signal will have compared to other GNSS signals. Whether these dynamics are due to platform motion, oscillator instability, or ionospheric variation, the cost to benefit the comparison of adding the necessary RF bandwidth, processing throughput, and associated power draw to a receiver could be called into question.

Other recent works such as Borio and Susi (2019) and Susi and Borio (2020) provide viable solutions to the signal tracking issues presented for users wishing to track the high symbol rate portion of the E6 signal without the benefit of pilot tracking. These solutions involve leveraging inter-signal aiding from the more robust signals broadcast from the satellite such as E1 or E5. With the information collected by the ARFIDAAS network regarding the relative occurrence rates of RFI on different GNSS signal bands, it can now be stated that such tracking schemes should take into account the observation that, when E6 is subjected to intentionally generated RFI (e.g., chirp) thought to come from PPD devices, the E1 band is frequently also targeted by a transmitted signal simultaneously. Conceptually, this makes sense as a jammer targeting only E6 would be ineffective against most GNSS receivers, but would still reduce the number of ways in which cooperative tracking between the E6 and other carriers might be employed within a receiver. The proposed use of other signals to track E6 within receivers is reminiscent of past tracking approaches adopted for semi-codeless L2 use and implies that similar secondary issues including ionospheric decorrelation and a lack of true frequency diversity in the event of jamming in the aiding bands would impact this approach. The full-year data from the five sites analyzed here indicates that such aiding of E6 would be least impacted by jamming if the aiding was provided by the E5a carrier. Use of the E5b carrier may be possible but, for three of the five stations, the level of RFI impacting E5b is likely much higher than the level impacting E5a as evidenced by the high level of Band C (1,203–1,263 MHz) time-modulated general events. Ongoing work includes updated analysis software that can produce reports based on specific signal bands of interest, in addition to the bands captured and shown here.

6 | FUTURE WORK

Presently, the deployed ARFIDAAS units send event-specific rapid analysis information with notification emails to site stakeholders, and centrally store collected raw complex signal samples along with these reports to the cloud service. Within 2022, it is planned to implement additional edge unit analysis as well as centralized processing within the cloud that will produce daily and monthly site reports to allow the collection of per site statistical summaries of the likelihood of encountering RFI within each band. Sites that presently have L2, L5, or E6 band detection disabled will need to be re-evaluated to determine the true rate of occurrence in the non-L1 bands, or the parameters available may be reduced to calculating the likelihood of multiband RFI impacting a system when L1-band RFI is present. This latter information will still be useful when considering the availability level of the discussed aided tracking strategies that might employ an L1 carrier to aid in the tracking of the E6 signal, but would not provide valid information for the potential aiding of E6 with one of the E5 signal components.

An example of information expected to be provided within the monthly reporting is which signal bands and signal band combinations were impacted throughout the month. Additional parameterization of the analysis software will allow isolation

of reporting to events that overlay defined sub-bands commensurate with specific signals or signal components, with which modulation types and at what relative power levels. Additional information on the design of the quad-band ARFIDAAS front-end and software systems can be found in Morrison et al. (2020), while information on the ongoing ARFIDAAS follow-on project underway between SINTEF and the University of Helsinki, which will leverage machine learning techniques to attempt to uniquely identify jamming devices in support of enforcement, will be published in the near future.

7 | CONCLUSION

Due to the encryption of some signal components of E6 (EU, 2019), recovering the data from the remaining unencrypted signal component may pose a challenge in the presence of any perturbing interference sources. Time-frequency adaptive filtering to address narrowband amateur radio and short pulse-length radar signals may be necessary to ensure robust operation of E6 in many regions of Europe. In other regions where wideband continuous emissions are permitted in an overlapping band, no amount of filtering may be sufficient to allow reasonable use of the E6 signal, regardless of whether they are authorized to track the encrypted pilot and Galileo's public regulated service (PRS), or not.

If dynamic aiding approaches are adopted by receiver manufacturers to permit the reliable exploitation of the data component of the E6 signal for non-authorized users, it can be expected to mitigate the issues caused by the small tracking margin. However, this will come with the cost of reintroducing drawbacks previously experienced before the availability of civil signals on carriers other than L1. While there will still be value to users trying to exploit the contents of the high-rate data message carried by E6, the message contents should be sufficiently redundant in the context of frequent loss of data to be practically useful.

While we have primarily focused on the signal tracking concerns posed for non-authorized users of the E6 signal high-accuracy and commercial authentication services (European GNSS Agency, 2020), since the relative vulnerability of this user segment is higher, some of the threats discussed will seriously disrupt the E6-A signal (PRS) as well. In cases where the signature of the interfering signal is pulsed (e.g., radar), pulse blanking or time-frequency strategies used for mitigation of distance measuring equipment (DME) type interference on the L5/E5 bands could be employed. Mitigation techniques such as adaptive notching may mitigate static narrowband sources such as amateur radio, but the remaining category of high-power, persistent, and wide-bandwidth RFI sources cannot be so directly addressed. Sources such as amateur TV transmissions covering several megahertz of spectrum or electronic warfare exercises saturating the entirety of the band will leave receiver designers with fewer options for mitigation, and even with access to the encrypted pilot and dynamic aiding, the signal will still be lost. Classifying GNSS as the primary user of the frequency band (1,215–1,300 MHz) is not sufficient as it does not prevent interference (ITU-R, 2019). Either the frequency band is allocated exclusively to GNSS without exceptions, or stricter guidelines must be adopted to allow interference-free coexistence of multiple users.

Comparison of the full-year data set parameters to the constituent month sub-periods exposes a high level of variability in the month-to-month data, such that individual band activity in all bands except L1/ E1 have been observed to increase or decrease by an order of magnitude between adjacent months. In terms of band-occupancy and modulation types, even at year-long periods, the RFI

environment at a given site can still be heavily influenced by a small number of PPD operators or other persistent sources in the local environment. Regrettably, none of the five monitored locations have shown activity levels lower than an average of several seconds per day of RFI. While presently the E1/L1 band is more frequently impacted by RFI from mobile PPD jammers, fixed sources of co-authorized user interference appear to be more common in the E6 band than in others.

The high concentration of narrowband jamming within the E1/L1 band is presently believed to be due to low cost or poorly designed active GNSS receivers leaking energy in their operating band. This prediction can be tested by observing the trend of narrowband event counts in the annual data as more multi-frequency low-cost receivers enter the market in coming years.

ACKNOWLEDGMENTS

The authors would like to thank the European Space Agency (NAVISP program) and the Norwegian Space Agency for funding the development of the ARFIDAAS, as well as the Norwegian Council of Research for funding system deployment activities. Additional thanks to the hosts of ARFIDAAS monitoring stations for their assistance.

Endnotes: Data collected by the ARFIDAAS is available to interested academic/research and commercial entities. While event data is stored in a format developed specifically for the ARFIDAAS project, decoders for conversion to raw binary are available. Representation of the data in other formats such as the 'Global Navigation Satellite Systems Software Defined Radio Sampled Data Metadata Standard' can be supported on request. Interested parties should contact one of the authors from SINTEF or the University of Helsinki for more information concerning event data. For information concerning monthly and annual analysis products focused on specific signals, bands, or combinations, please contact one of the SINTEF authors.

REFERENCES

Arribas, J., Vilà-Valls J., Ramos, A., Fernández-Prades, C., & Closas, P. (2019). Air traffic control radar interference event in the Galileo E6 band: detection and localization. *NAVIGATION*, *66*(3), 505–522. https://doi.org/10.1002/navi.310

Borio, D., & M. Susi. (2019). Working paper: processing options for the E6B signal. *Inside GNSS*, *14*(3), 40–47. https://insidegnss.com/working-paper-processing-options-%E2%80%A8for-the-e6b-signals/

Curran, J., & Melgard, T. (2016). The particular importance of Galileo E6C. *Inside GNSS*, *11*(5), 57–63. https://insidegnss.com/the-particular-importance-of-galileo-e6c-2/

de Bakker, P.F. (2007). Effects of radio frequency interference on GNSS receiver output [Master's Thesis, Delft University of Technology Faculty of Aerospace Engineering]. https://docplayer.net/21352811-Effects-of-radio-frequency-interference-on-gnss-receiver-output-masters-thesis-peter-f-de-bakker.html

Diez, A., Morrison, A., & Sokolova, N. (2022a). Automatic classification of RFI events from a multi-band multi-site GNSS monitoring network. *Proc. of the 35th International Technical Meeting of the Satellite Division of the Institute of Navigation (ION GNSS+ 2022)*, Denver, CO, 3907–3914. https://doi.org/10.33012/2022.18572

Diez, A., Morrison, A. J., & Sokolova, N. (2022b). Automatic GNSS RFI classification challenges. *European Journal of Navigation*, *22*(2), 12–21. https://www.sintef.no/en/publications/publication/2050861

European GNSS Agency. (2020). Galileo high accuracy service (HAS) [Info note]. https://www.gsc-europa.eu/sites/default/files/sites/all/files/Galileo_HAS_Info_Note.pdf

European Union (EU). (2019). *Galileo E6-B/C codes* [Technical note]. https://www.gsc-europa.eu/sites/default/files/sites/all/files/E6BC_SIS_Technical_Note.pdf

European Union (EU). (2021). *European GNSS (Galileo) open service signal-in-space interface control document issue 2.0* [Technical report]. https://www.gsc-europa.eu/sites/default/files/sites/all/files/Galileo_OS_SIS_ICD_v2.0.pdf

International Telecommunication Union (ITU-R). (2019). *Characteristics and protection criteria for receiving Earth stations in the radionavigation-satellite service (space-to-Earth) operating in the band 1,215–1,300 MHz* [Recommendation ITU-R M.1902-1]. https://www.itu.int/dms_pubrec/itu-r/rec/m/R-REC-M.1902-1-201909-I!!PDF-E.pdf

JAXA. (2014). *Advanced Land Observing Satellite (ALOS-2) overview*. https://www.eorc.jaxa.jp/ALOS/en/alos-2/a2_about_e.htm

Julien, O., & Macabiau, C. (2006). New GNSS frequencies, advantages of M-Code, and the benefits of a solitary Galileo satellite. *Inside GNSS*, *1*(4), 22–25. https://insidegnss-com.exactdn.com/wp-content/uploads/2018/01/MayJune06GNSSSolutions.pdf

Lynum, S. (2020). *Trener på elektronisk krigføring – kan forstyrre navigasjon i bil log mobiltelefoner*. https://www.adressa.no/nyheter/trondelag/2020/02/24/Trener-p%C3%A5-elektronisk-krigf%C3%B8ring-kan-forstyrre-navigasjon-i-bil-og-mobiltelefoner-21163474.ece

Morrison, A. J., & Sokolova, N. (2021). Multi-band multi-site GNSS RFI monitoring results after a year of operation. *European Journal of Navigation, 21*(3), 4–15. https://www.sintef.no/en/publications/publication/1974702

Morrison, A. J., Sokolova, N., Gerrard, N., Rødningsby, A., Rost, C., & Ruotsalainen, L. (2021). RFI considerations for utility of the Galileo E6 signal. *Proc. of the 34th International Technical Meeting of the Satellite Division of the Institute of Navigation (ION GNSS+ 2021)*, St. Louis, MO, 2870–2878. https://doi.org/10.33012/2021.18018

Morrison, A., Sokolova, N., Håkegård, J. E., Bryne, T. H., & Ruotsalainen, L. (2020). A multi-site quad-band radio frequency interference monitoring alerting and reporting system. *2020 European Navigation Conference (ENC GNSS)*, Dresden, Germany. https://doi.org/10.23919/ENC48637.2020.9317522

Pullen, S., Gao, G., Tedeschi, C., & Warburton, J. (2012). The impact of uninformed RF interference on GBAS and potential mitigations. *Proc. of the 2012 International Technical Meeting of the Institute of Navigation*, Newport Beach, CA, 780–789. https://www.ion.org/publications/abstract.cfm?articleID=9992

Schuster, W., & Ochieng, W. (2010). Harmonisation of Category-III precision approach navigation system performance requirements. *The Journal of Navigation*, *63*(4), 569–589. https://doi.org/10.1017/S0373463310000287

Schütz, A., Kraus, T., Lichtenberger, C. A., & Pany, T. (2021). A case study for potential implications on the reception of Galileo E6 by amateur radio interference on German highways considering various transmitter-receiver-signal combinations. *Proc. of the 34th International Technical Meeting of the Satellite Division of the Institute of Navigation (ION GNSS+ 2021)*, St. Louis, MO, 1687–1696. https://doi.org/10.33012/2021.18026

Susi, M., & Borio, D. (2020). Kalman filtering with noncoherent integrations for Galileo E6-B tracking. *NAVIGATION*, *67*(3), 601– 617. https://doi.org/10.1002/navi.380

Towlson, O., Payne, D., Eliardsson, P., & Manikundalam, V. (2019). *Standardisation of GNSS threat reporting and receiver testing through international knowledge exchange, experimentation and exploitation* [STRIKE3-D6.2: Threat database analysis report]. https://aric-aachen.de/strike3/downloads/STRIKE3_D6.2_Threat_database_Analysis_Report_public_v1.0.pdf

Van Hees, J. (2016). GPS/GNSS interference mitigation. *56th Meeting of Civil GPS Service Interface Committee (CGSIC) GNSS+ 2016 Conference,* Portland, OR. https://www.gps.gov/cgsic/meetings/2016/vanhees.pdf

How to cite this article: Morrison, A., Sokolova, N., Gerrard, N., Rødningsby, A., Rost, C., & Ruotsalainen, L. (2023). Radio-frequency interference considerations for utility of the Galileo E6 signal based on long-term monitoring by ARFIDAAS. *NAVIGATION, 70*(1). https://doi.org/10.33012/navi.560